Carbohydrate Polymers 322 (2023) 121367

Contents lists available at ScienceDirect

Carbohydrate Polymers

journal homepage: www.elsevier.com/locate/carbpol

Investigation of the structural and immunomodulatory properties of alkali-soluble β-glucans from *Pleurotus eryngii* fruiting bodies

Christiane F. Ellefsen [a,*], Linda Lindstad [a], Leesa J. Klau [b], Finn L. Aachmann [b], Marianne Hiorth [a], Anne Berit C. Samuelsen [a]

[a] Department of Pharmacy, University of Oslo, Sem Sælands vei 3, 1068 Blindern, NO-0371 Oslo, Norway
[b] Department of Biotechnology and Food Science, NTNU Norwegian University of Science and Technology, Sem Sælands vei 6/8, NO-7491 Trondheim, Norway

ARTICLE INFO

Keywords:
Mushroom glucans
NMR
Dispersion
Dectin-1
THP-1

ABSTRACT

Fungal β-glucans have received a lot of interest due to their proinflammatory activity towards cells of the innate immune system. Although commonly described as (1➔3)-β-glucans with varying degree of (1➔6)-branching, the fungal β-glucans constitute a diverse polysaccharide class. In this study, the alkali-soluble β-glucans from the edible mushroom *Pleurotus eryngii* were extracted and characterized by GC, GC–MS and 2D NMR analyses. The extracts contain several structurally different polysaccharides, including a (1➔3)-β-D-glucan with single glucose units attached at *O*-6, and a (1➔6)-β-D-glucan, possibly branched at *O*-3. The immunomodulatory activities of the *P. eryngii* extracts were assessed by investigating their ability to bind to the receptor dectin-1, and their ability to induce production of the proinflammatory cytokines TNF-α, IL-6 and IL-1β in LPS-differentiated THP-1 cells. Although the samples were able to bind to the dectin-1a receptor, they did not induce production of significant levels of cytokines in the THP-1 cells. Positive controls of yeast-derived (1➔3)-β-D-glucans with branches at *O*-6 induced cytokine production in the cells. Thus, it appears that the *P. eryngii* β-glucans are unable to induce production of proinflammatory cytokines in LPS-differentiated THP-1 cells, despite being able to activate the human dectin-1a receptor.

1. Introduction

Fungal β-glucans are well-known immunomodulatory compounds that elicit a proinflammatory response from cells of the innate immune system. Therefore, fungal β-glucans have been suggested to be used as adjuvants in cancer treatments or vaccines, and as treatment against infections (dos Santos et al., 2019; Graubaum et al., 2012; Vetvicka et al., 2020). Their typical structural features are described as (1➔3)-β-D-glucans, with branches of β-(1➔6)-linked glucan residues at *O*-6 to varying extents. The fungal cell wall also consist of other β-glucans, with (1➔6) or (1➔4)-linked backbones and/or (1➔3), (1➔2) or (1➔4)-linked branches (Ruiz-Herrera & Ortiz-Castellanos, 2019; Synytsya & Novák, 2013). Additionally, different α-glucans have been reported from fungal sources, the most typical of which are the (1➔3)-α-D-glucans and the glycogen-like (1➔4),(1➔6)-α-D-glucans, as further elaborated in the review by Synytsya and Novák (2013).

Most research conducted towards the biological activity of fungal β-glucans has revolved around β-glucans isolated from baker's yeast (*Saccharomyces cerevisiae*). Zymosan is one such *S. cerevisiae*-derived product, consisting of a (1➔3)-β-glucan backbone with branches at *O*-6, mixed with non-glucan entities such as mannan and protein (Di Carlo & Fiore, 1958). Zymosan has been shown to elicit a proinflammatory response through binding to both the c-type lectin receptor dectin-1, Toll-like receptor 2 (TLR2) and TLR4 (Brown et al., 2003; Ferwerda et al., 2008; Gantner et al., 2003). Dectin-1 has been identified as a major receptor responsible for β-glucan activity on some immune cells, such as macrophages and dendritic cells. Another fungus that has been studied in-depth is the Basidiomycota shiitake (*Lentinus edodes*). Shiitake contains lentinan, a (1➔3)-β-D-glucan with single glucose units attached at *O*-6, which has been the subject of several trials, including clinical studies as adjuvant treatment in cancer therapy, as summarized by Zhang et al. (2011) in their review.

A large number of β-glucans from other fungal sources have been studied over the last decades. However, regarding their biological activity, the results are often not concurring, and a consensus to the link between structure and activity has not been reached (Han et al., 2020;

* Corresponding author.
E-mail address: c.f.ellefsen@farmasi.uio.no (C.F. Ellefsen).

https://doi.org/10.1016/j.carbpol.2023.121367
Received 29 June 2023; Received in revised form 25 August 2023; Accepted 4 September 2023
Available online 9 September 2023

Williams et al., 1996). The polymer structure is believed to be important for dectin-1 binding and proinflammatory activation, and several studies have attempted to elucidate this. For instance, the (1➔3),(1➔4)-β-glucans from cereals are structurally related to the fungal β-glucans, but lack the proinflammatory properties that the (1➔3),(1➔6)-glucans possess (Han et al., 2020). Similarly, (1➔6)-β-glucans from fungi have been shown to lack the same proinflammatory activity. Cereal β-glucans, (1➔6)-β-glucans and (1➔3)-β-glucans with less than seven units in the main chain have been shown not to interact with murine dectin-1 (Adams et al., 2008). However, in other studies, both cereal β-glucans and (1➔6)-linked fungal β-glucans have been reported to stimulate the release of proinflammatory cytokines from immune cells (Rösch et al., 2016). These diverging results highlight the need for more studies regarding the true nature of how the immunomodulatory properties of fungal β-glucans relate to their structures. This also requires thorough structural elucidation of the glucans that are tested.

Pleurotus eryngii, the king oyster mushroom, is a mushroom that is easily cultivated and has been shown to contain both α- and β-glucans (Abreu et al., 2021). We have previously investigated the water-soluble polysaccharides of *P. eryngii*, and found that they do not possess any significant ability to activate dectin-1, TLR2, or mouse D2SC/1 dendritic cells (Ellefsen et al., 2021). The aim of this new study was to elucidate the structures and assess the immunomodulatory properties of alkali-soluble polysaccharides of this mushroom, as we hypothesized that *P. eryngii* contains poorly water-soluble β-glucans with activity towards dectin-1, as well as immunomodulatory activity.

2. Experimental

2.1. Materials

Fresh *P. eryngii* fruiting bodies were purchased from Trøndersopp (Verdal, Norway, www.trondersopp.no) and identified by Prof. Klaus Høiland at the Section for Genetics and Evolutionary Biology, University of Oslo. *S. cerevisiae* derived particulate β-glucans zymosan A (ZymA) and zymosan depleted (ZymD) were purchased from Sigma-Aldrich (St. Louis, MO, USA) and InvivoGen (www.invivogen.com, Toulouse, France), respectively. The *S. cerevisiae* glucan Wellmune WGP Dispersible powder (BG-P; Lot 09240-04; Biothera, Eagan, MN, USA) was kindly provided from Immitec, Tønsberg, Norway. The soluble *Laminaria digitata* β-glucan laminarin (Lam) was purchased from Sigma-Aldrich, Norway.

2.1.1. Extraction

Lyophilized and milled *P. eryngii* fruiting bodies (150 g) were submitted to a sequential extraction procedure using solvents of increasing polarities as described in Ellefsen et al. (2021). The residue from water extraction was first treated with 1200 mL 0.1 M NaOH containing 0.104 M $NaBH_4$ and 20 mL 1-octanol, under reflux for 3 h (PeA1). The process was repeated, first with 1000 mL 0.5 M NaOH (PeA2) and then with 1000 mL 1.0 M NaOH (PeA3), in both cases with 0.135 M $NaBH_4$ and 30 mL 1-octanol added, and over 4 h. The alkaline extracts were precipitated with 3 volumes of EtOH at 4 °C overnight. The precipitates were washed thrice with 70 % EtOH, dialyzed against distilled water (Mw cut-off 12–14 kDa, SpectraPor® Dialysis membrane, Spectrum Chemical Mfg. Corp., New Brunswick, NJ, USA) and lyophilized.

2.2. Polysaccharide characterization

2.2.1. Monosaccharide composition

Methanolysis, TMS-derivatization and subsequent GC-FID analysis of the alkaline extracts were performed as previously described by Nyman et al. (2016). A Restek-Rtx-5 silica column (30 m, i.d. 0.25 mm, 0.25 μm film thickness) coupled to a Focus GC (Thermo Scientific, Waltham, MA, USA) was utilized, with split (1/10) injection at constant pressure mode and helium as the carrier gas. The injector and detector temperatures were set to 250 and 300 °C, respectively, while the column temperature was 140 °C upon injection. After injection, the column temperature was increased by 1 °C/min to 150 °C, held for 3 min, increased by 3 °C/min to 170 °C, held for 5 min, increased by 15 °C/min to 310 °C, and held for 3 min. Chromatograms were analyzed using the Chromelion v.6.80 (Dionex Corporation, Sunnyvale, CA, USA) software.

2.2.2. Linkage analysis

Samples PeA2 and PeA3 (1–2 mg) were washed with anhydrous methanol (200 μL) and dried with N_2 (g) twice, before drying over P_2O_5 overnight. DMSO (500 μL) was then added under N_2 atmosphere. The samples were heated to 80 °C for 30–60 min and then shaken for 30–60 min repeatedly, before being left at 4 °C overnight. Methylation and hydrolysis were conducted and included a formic acid pre-hydrolysis step, as recommended for less water-soluble polysaccharides, followed by reduction and acetylation as described by Pettolino et al. (2012). The products were analyzed on a GC–MS-QP2010 (Shimadzu Corporation, Kyoto, Kyoto, Japan) using a Restek Rxi-5MS silica column (30 m, i.d. 0.25 mm, 0.25 μm film thickness) using split injection at constant pressure mode. Helium was the carrier gas, the initial flow was at 1 mL/min, and the interface temperature was 280 °C. The column temperature was 80 °C upon injection and held for the first 5 min, before an increase by 10 °C/min to 140 °C, then by 4 °C/min to 210 °C, then by 20 °C/min to 310 °C, and held for 4 min. The ion source temperature was 200 °C. Spectra were analyzed using GC–MS solution v.2.10 (Shimadzu Corporation) software.

2.2.3. Dispersion

Due to low water-solubility of PeA2 and PeA3, different dispersion methods were attempted before samples were subjected to the phenol/sulfuric acid assay. The samples PeA2 and PeA3 were left swelling in water at 4 °C overnight, before milling at 25,000 rpm for 5 min, using a T25 digital Ultra-Turrax® (Ika, Staufen, Germany) equipped with an S 25 N-8-G-ST tip (Ika). Another batch of samples were milled and then left swelling at 4 °C overnight.

Dispersion was also attempted by dissolving 25 mg sample in 5 mL 1 M NaOH by heating at 60 °C for 15–20 min, followed by dilution (1:1) and precipitation by dropwise addition into a stirring solution of 10 mL 0.5 M HCl. The same method was applied for sample preparation before conducting reporter cell line assays.

For THP-1 cell experiments, a similar method was applied, but only with PeA3, and with 10× or 40× dilution before precipitation. The resultant samples, PeA3-PI (10× dilution) and PeA3-PII (40× dilution) were lyophilized.

2.2.4. Total carbohydrate content

The total carbohydrate contents of samples PeA2 and PeA3 were determined using the phenol/sulfuric acid assay (DuBois et al., 1956) using a D-glucose standard curve and absorbance measurements at 490 nm. Measurements were performed in triplicates.

2.2.5. Elemental analysis

Sulfur, nitrogen and carbon were measured by elemental analysis via total combustion using a Vario-EL cube elemental analyzer (Elementar Analysensysteme GmbH, Langenselbold, Germany). Nitrogen contents (% of dry weight) were calculated as the mean of two measurements, and protein contents were estimated by the formula %N × protein factor 6.25.

2.2.6. Dynamic light scattering (DLS)

Lyophilized PeA3-PI and PeA3-PII were resuspended in milli-Q® water (18.2 Ω) and sonicated for 40 s at 40 % amplitude, using a Vibra cell™ VCX 130 W ultrasonic processor (Sonics & Materials Inc., Newtown, CT, USA) with a 3 mm tapered microtip (Sonics & Materials Inc.). Samples were measured by dynamic light scattering (DLS) using a Zetasizer Nano ZS (Malvern Instruments Ltd., Worcestershire, UK). The

measurements were performed using backscatter detection at 173° at 25 °C. The refractive index and viscosity were set to those of pure water. Polystyrene latex particles were given as the material setting. The particle size (Z-average) and polydispersity index (PDI) were obtained using the cumulant fit model. Measurements were made after a temperature equilibration time of 300 s.

2.2.7. NMR

Samples (15 mg) were dissolved in 600 μL DMSO-d_6 by heating at 60 °C for 2 h. The samples were sonicated for 5 min, filtered, and transferred to 5 mm diameter NMR-tubes. Initially, ^{1}H (*zg30*) and HSQC (*hsqcedetgpsisp2.3* TD(F2) 2048, TD(F1) 256, NS 8) experiments were recorded for all three samples on a Bruker Avance NEO 600 MHz spectrometer, at 80 °C. D_2O *d*-99.9 % (10 %) was added to the NMR tube of PeA3, and the following experiments were recorded on a Bruker Ascend HDIII 800 MHz spectrometer at 60 °C: ^{1}H (w/NOESY presaturation for solvent suppression, *noesygppr1d*, TD 65536, NS 16, expt 2 min), ^{13}C (*zgpg30_baseline*, TD 131072, NS 8192), HSQC (*hsqcedetgpsisp2.3*, TD(F2) 2048, TD(F1) 512, NS 8, expt 2.5 h), HMBC (*hmbcetgpl3nd*, TD(F2) 2048, TD(F1) 512, NS 24, expt 7.5 h), H2BC (*h2bcetgpl3pr*, TD(F2) 2048, TD(F1) 512, NS 32, expt) and HSQC-TOCSY (*hsqcdietgpsisp.2*, TD(F2) 2048, TD(F1) 400, NS 24, d9 70 ms, expt 6 h). Additionally, a diffusion ordered spectroscopy experiment (DOSY; *dstebpgp3spr*, TD(F2) 32768, TD(F1) 32, NS 32, p30 (δ) 2 ms, d20 (Δ) 0.2 s, 5–85 % gradient strength) was recorded. A 2D NOESY experiment (*noesyesgpph*, TD(F2) 4096, TD(F1) 800, NS 32, d8 80 ms, expt 11 h) was recorded at 50 °C on the same spectrometer. The chemical shifts were referenced to DMSO (^{1}H: 2.50 ppm; ^{13}C: 39.51 ppm). Spectra were processed and analyzed using TopSpin 3.6.2.

2.2.8. Determination of lipopolysaccharide (LPS) content in β-glucan samples

The content of lipopolysaccharide (LPS) in the samples (PeA2, PeA3) and β-glucan references BG-P and laminarin (Lam; Sigma-Aldrich) was determined through derivatization into 3-*O*-acetyl fatty acid methyl esters followed by GC–MS analysis, as described by de Santana-Filho et al. (2012). Briefly, 300 μL anhydrous methanol and 200 μL 3 M HCl in anhydrous methanol were added to 3–5 mg of each sample. The samples were vortexed gently and heated at 80 °C for 20 h. After this, 500 μL H_2O was added and the fatty acid methyl esters were extracted with 3 × 1 mL *n*-hexane. The hydroxyl-fatty acid methyl esters were then acetylated by addition of acetic anhydride in pyridine for 1 h at 100 °C. The samples were dried, and then dissolved in 100 μL acetone before analysis on a GCMS-QP2010 (Shimadzu Corporation) using a Restek Rxi-5MS silica column (30 m, i.d. 0.25 mm, 0.25 μm film thickness), with split injection and constant pressure mode. Helium was the carrier gas, the initial flow was 1 mL/min, and the interface temperature was 250 °C. The column temperature was 60 °C upon injection and for the following 1 min. Then, a 20 °C/min temperature increase until 110 °C was followed by a 5 °C/min increase until the temperature reached 240 °C. Finally, the temperature was increased by 20 °C/min until reaching 310 °C, where it was kept for 1 min. The ion source temperature was 200 °C. Spectra were analyzed using GC–MS solution v2.10 software (Shimadzu Corporation).

2.3. Bioassays

2.3.1. HEK-Blue™ reporter cell line assays

The HEK-Blue™ hDectin-1a (InvivoGen) reporter cell line and the HEK-Blue hNull1-v (InvivoGen) parental cell line, were cultured in Dulbecco's modified Eagles medium (DMEM; Gibco, Bleisweijk, The Netherlands) supplemented with 10 % fetal bovine serum (FBS; Gibco), 1 % PenStrep (Gibco) and 100 μg/mL Normocin™ (InvivoGen). The selection antibiotics Puromycin (100 μg/mL; InvivoGen) and HEK-Blue™ CLR Selection (1×; InvivoGen) were added for the hDectin-1a cell line, while Zeocin™ (100 μg/mL; InvivoGen) was added for the hNull1-v cells. Cells were passaged 2–3 times a week and maintained at <90 % confluency.

PeA2 and PeA3, dispersed through precipitation (see Section 2.2.4), were added to a 96-well microtiter plate in 20 μL triplicates. Lam (30 μg/mL), and ZymD (10 μg/mL) were added as positive controls for the dectin-1a cells, while TNF-α (100 ng/mL; Thermo Fischer) was used as a positive control with the Null1-v cells. Milli-q water was included as a negative control with both cell lines. Cells were harvested using phosphate buffer saline (PBS; Gibco), as advised by the manufacturer, and diluted to 280,000 cells/mL with HEK-Blue™ detection medium (InvivoGen), such that addition of 180 μL cell suspension to each well corresponded to 50,000 cells/well. The plates were incubated in a humid incubator at 37 °C with 5 % CO_2 for 16 h. Cell supernatants were transferred to new plates, and the absorbance at 635 nm was recorded. The cell experiment was executed three times for each of the cell lines.

2.3.2. THP-1 culturing, differentiation and stimulation

The human monocytic cell line THP-1 (ATCC, Manassas, VA, USA) was cultured in RPMI 1640 medium (Gibco) supplemented with 10 % fetal bovine serum (FBS; Gibco). The cells were passaged 1–2 times a week and maintained at $<1.0 \times 10^6$ cells/mL.

THP-1 human monocytes were seeded in 96 well plates (625,000 cells/mL, 80 μL), and differentiated into macrophage (Mφ)-like cells by addition of 500 ng/mL LPS (20 μL) for 24 h. The LPS-containing medium was removed, and the cells were washed gently with PBS, before 100 μL LPS-free growth medium (RPMI 1640, containing 10 % FBS) was added, and the cells were incubated for 24 h.

The Mφ-like cells were stimulated with samples and controls for 20 h. The lyophilized samples PeA3-PI, PeA3-PII (see Section 2.2.4) and PeA3 were resuspended in water and sonicated for 20 s at 40 % amplitude. Further dilutions were made with growth medium, and the samples were then added to the cells at 100, 10 and 1 μg/mL, in triplicates. The yeast-derived β-glucans ZymA (10 μg/mL), ZymD (100 μg/mL), and BG-P (100 μg/mL), along with Lam (100 μg/mL; Sigma-Aldrich), were also included. As a non-β-glucan positive control 500 ng/mL lipopolysaccharide (LPS, from *Escherichia coli*, 055:B5, Sigma-Aldrich) was also included. The cells were incubated at 37 °C in a humid incubator containing 5 % CO_2. The actin polymerization inhibitor cytochalasin D (CytD; from *Zygosporium mansonii*; Sigma-Aldrich) was added 30 min prior to stimulation and maintained at 2.5 μM concentration (Hernanz-Falcón et al., 2009). The experiment was performed three times in total.

2.3.3. Cytokine detection

The content of the human proinflammatory cytokines TNF-α, IL-6 and IL-1β in THP-1 cell supernatants was determined using DuoSet ELISA kits (Bio-Techne, Minneapolis, MN, USA). The kits were used at halved volumes in half-area 96-well plates, but otherwise as instructed by the manufacturer.

2.3.4. Cell viability assay

The viability of the THP-1 cells stimulated with samples and controls was determined using the MTT assay (Cell Proliferation Kit I, Roche). After removal of the cell supernatants 100 μL growth medium was added to the cells and they were incubated for 1 h in a humid incubator with 5 % CO_2 at 37 °C. Then, 10 μL MTT-reagent (3-(4,5-dimethylthiazol-2-yl)-2,5-diphenyltetrazolium bromide) was added and the cells were incubated for another 4 h. The MTT-solubilizing reagent (100 μL) was then added, and the plate was left to incubate overnight before absorbance measurements at 570 and 690 nm. The viability of the cells was calculated based on subtracting A690 from A570 and compared with the A570-A690 difference of the untreated cells (100 % viability) and the cells treated with 33 % DMSO (0 % viability).

2.4. Statistical analysis

Data were expressed as the mean ± standard deviation. Significance

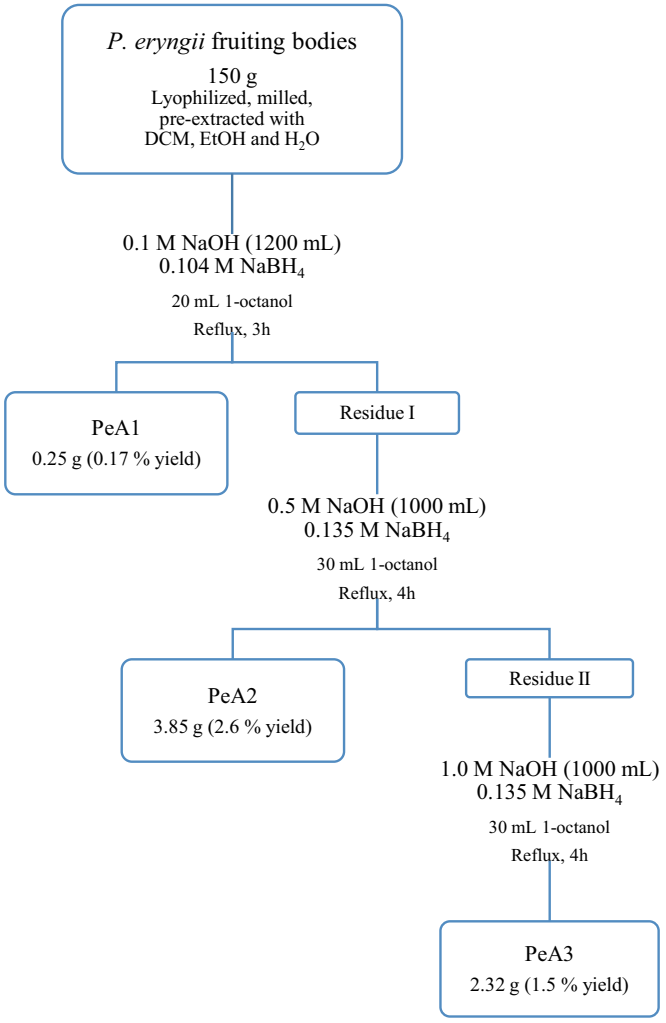

Fig. 1. Flowchart of the sequential extraction procedure that was followed to obtain the alkaline extracts PeA1, PeA2 and PeA3 from dried fruiting bodies of the mushroom *Pleurotus eryngii*.

Table 1
Monosaccharide compositions (w/w%) of the *P. eryngii* alkaline extracts PeA1, PeA2 and PeA3.

	Fuc	Xyl	Man	Gal	Glc	GlcA	GalA	3-*O*-Me Gal
PeA1	1	2	16	10	61	4	4	2
PeA2	<1	6	9	3	80	<1	<1	<1
PeA3	<1	2	6	2	89	<1	1	<1

Fuc, fucose; Xyl, xylose; Man, mannose; Gal, galactose; Glc, glucose; GlcA; glucuronic acid; GalA, galacturonic acid; 3-*O*-Me Gal, 3-*O* methyl galactose.

was determined using a one-way ANOVA with Dunnett's multiple comparisons test using GraphPad Prism v.9.3.1 (GraphPad Software, San Diego, CA, USA). $P < 0.05$ was considered statistically significant.

3. Results and discussion

3.1. Polysaccharide characterization

As shown in Fig. 1, the alkaline extraction resulted in the three alkaline extracts, PeA1, PeA2 and PeA3 with yields of 0.17 %, 2.6 % and 1.5 %, respectively. PeA1 was light brown-beige, while PeA2 and PeA3 were white. Otherwise, the three extracts were similarly cotton-like substances. All three samples contained glucose as their main carbohydrate component (Table 1). Out of the total carbohydrates, PeA1 contained only 61 % glucose, and relatively large amounts of mannose (16 %) and galactose (10 %). The mannose and galactose were likely remains of the water-soluble 3-*O*-methylated mannogalactan previously described (Ellefsen et al., 2021). Elemental analysis revealed that PeA1 contained approximately 8.4 % protein. Due to low content of glucose and the high protein content, PeA1 was not included for any further experiments.

Out of the total carbohydrates, PeA2 and PeA3 contained 80 % and 89 % glucose, respectively, indicating high contents of β-glucan. Furthermore, they were found to contain low amounts of protein: approximately 0.6 % and 1.0 %, respectively.

The initial results of the phenol/sulfuric acid assay indicated very low total carbohydrate contents of samples PeA2 and PeA3 (Table 2). This was probably due to low water-solubility of the samples. Limited water-solubility and aggregation of polysaccharides in the samples are likely to affect their availability for dehydration by sulfuric acid in the phenol/sulfuric acid assay, and thereby the formation of the final, colored complex.

Attempts were made to prepare more homogeneous dispersions to improve measurement accuracy and precision. Milling the samples followed by swelling overnight did not increase the measured carbohydrate content, whereas swelling overnight followed by milling did improve measurements, although standard deviations were relatively high. Dispersion through precipitation before the phenol/sulfuric acid assay resulted in the highest measured carbohydrate content of both samples: 94.7 ± 3.9 % and 84.5 ± 4.0 %, respectively. The lowered standard deviation indicated that this method yielded more homogeneous dispersions compared to the other methods. A dispersion of smaller particles, with larger surface-volume ratios may explain the improvement of the method.

The same linkage types were found in PeA2 and PeA3, but the relative abundance of the various linkages differed between the samples (Table 3). While PeA2 contained 26 % non-reducing end glucose, 19 % →3)-Glc*p*-(1→ and 25 % →6)-Glc*p*-(1→, PeA3 contained more of the →3)-Glc*p*-(1→ (36 %), and less →6)-Glc*p*-(1→ (20 %), and only 16 % non-reducing ends of glucose.

The HSQC spectra of PeA2 (presented in supplementary data) and PeA3 (Fig. 2A) were found to be very similar, the main difference being

Table 2
Total carbohydrate content (w/w%) of *P. eryngii* alkaline extracts PeA2 and PeA3 as determined using the phenol/sulfuric acid assay following various methods of sample dispersion. The presented numbers are the average and SD of five parallel measurements.

	No pretreatment	Milling – swelling	Swelling – milling	Precipitation
PeA2	49.2 ± 8.3	43.9 ± 2.5	90.1 ± 9.6	94.7 ± 3.9
PeA3	39.5 ± 7.2	36.4 ± 0.6	75.0 ± 8.4	84.5 ± 4.0

Table 3
Relative abundance of linkage types (% of total) found in the *P. eryngii* alkaline extracts PeA2 and PeA3.

Linkage type	PeA2	PeA3
Fuc*p*-(1→	<1	<1
Xyl*p*-(1→	4	1
→2)-Xyl*p*-(1→	2	1
→3)-Gal*p*-(1→	2	1
→6)-Gal*p*-(1→	<1	<1
→2,6)-Gal*p*-(1→	<1	<1
→3)-Man*p*-(1→	9	6
Glc*p*-(1→	26	16
→3)-Glc*p*-(1→	19	36
→6)-Glc*p*-(1→	25	20
→3,6)-Glc*p*-(1→	11	17

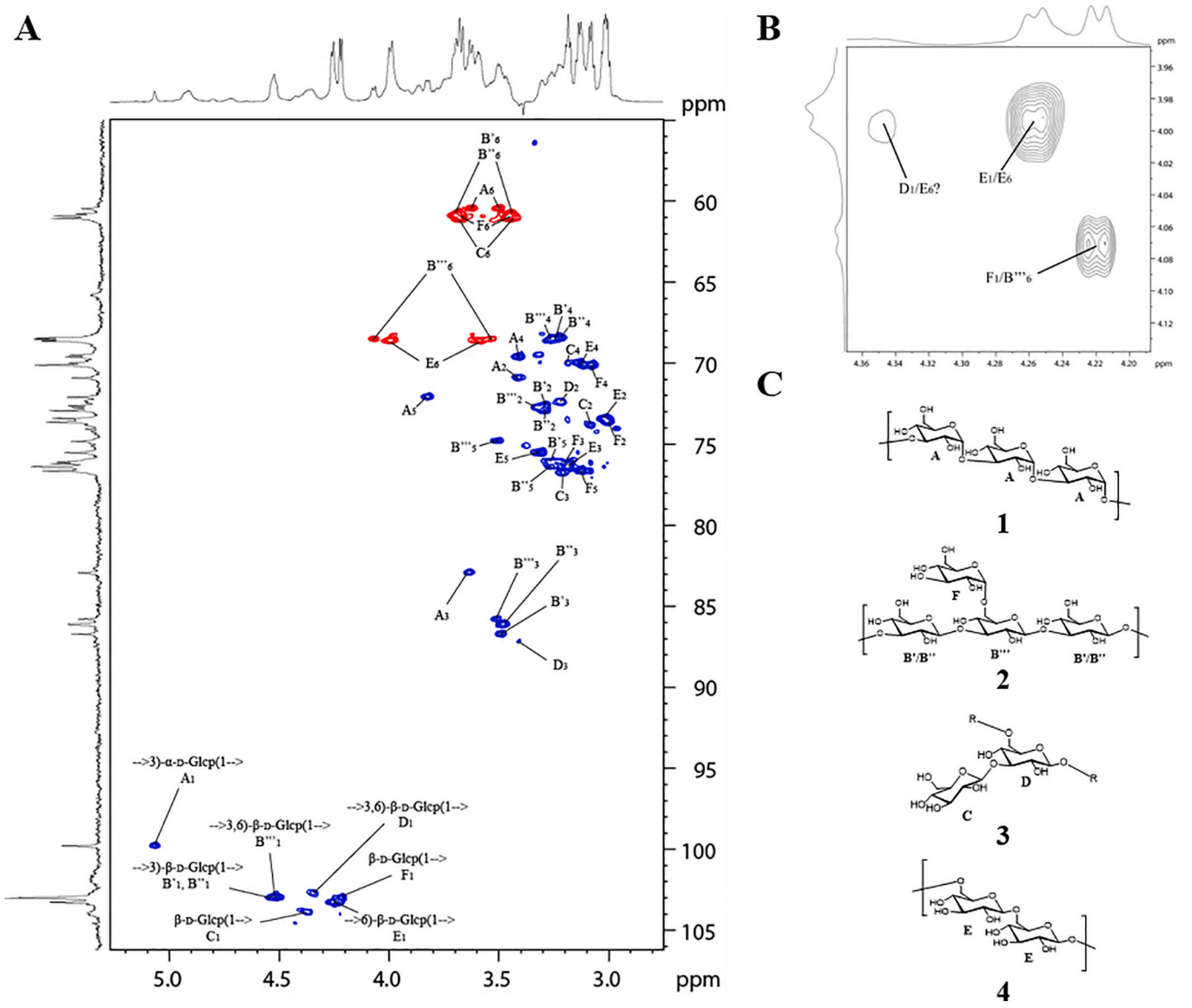

Fig. 2. NMR spectra of PeA3 in 90 % DMSO-d_6 recorded on a Bruker Ascend HDIII 800 MHz spectrometer at 60 °C, with markings of cross peaks from residues A-F. A DEPT-135 edited HSQC, B NOESY spectrum close-up C Suggested structures of alkali-soluble *P. eryngii* glucans: a linear (1➔3)-α-D-glucan ., a (1➔3)-β-D-glucan branched at *O*-6 with single glucose residues **2** and the two fragments **3** and **4**, possibly making up a (1➔6)-β-D-glucan branched with single glucose residues attached at *O*-3. The chemical shifts were referenced to DMSO.

the presence of some α-glucan signals in PeA3 that were absent in PeA2. The structure elucidation of the *P. eryngii* alkaline extracts was therefore based upon the spectra of PeA3, as this sample also contained the highest relative amount of glucose. In the DEPT135-edited HSQC spectrum, five main cross peaks were found in the anomeric region. These were assigned to glucose residues with different linkage positions using correlations found in the HMBC, H2BC, HSQC-TOCSY and NOESY spectra (Fig. 2B and supplementary data), as well as through comparison to reference spectra, as described in the following paragraphs. Correlations and assignments of all residues are presented in Table 4.

The anomeric signals appearing from the typical fungal ➔3)-β-D-Glc*p*-(1➔ (residue B) and ➔6)-β-D-Glc*p*-(1➔ (residue E) were found at 4.53/103.4 ppm and 4.27/103.7 ppm, respectively. In addition, the *H*-1/*C*-1 cross-peaks of non-reducing end β-D-Glc*p*-(1➔ (residues C and F) were identified at 4.38/104.3 and 4.23/103.4 ppm, while ➔3,6)-β-D-Glc*p*-(1➔ (residue D) appeared at 4.35/103.1 ppm. An anomeric signal was visible in the α-region, at 5.08/100.2 ppm. This was identified as ➔3)-α-D-Glc*p*-(1➔ (residue A) through comparison to reference spectra (Ellefsen et al., 2021, supplementary data). The remaining signals of each residue were assigned as follows: From A_1, H2BC correlations were found to the signal at 3.42/71.3 ppm, which was assigned as A_2. Additionally, HMBC correlations to 3.64/83.4 ppm and 3.83/72.5 ppm indicated that these signals belonged to A_3 and A_5, of which the former was identified as A_3 due to H2BC correlations with A_2. Furthermore, the higher ^{13}C chemical shift indicated that A_3 participated in a glycosidic linkage. The cross peak appearing from A_4 was found at 3.42/70.1 ppm, with H2BC correlations to both A_3 and A_5, and HMBC correlations to A_3, A_5, and A_6, which was identified as the signals at 3.64 & 3.51/60.9 ppm.

The anomeric signal of residue B at 4.52–4.54/103.4 ppm shared H2BC correlations with the signal cluster at 3.30–3.39/73.1–73.3 ppm, splitting the residue into three, B′, B″ and B‴. All three residues were found to participate in (1➔3)-glycosidic linkages, as they shared HMBC correlations with the signal cluster at around 3.49–3.52/86.1–87.1 ppm. Inter residue correlations were identified between B'_1 and B'''_3, and B'''_1 and B'_3 in the HMBC spectrum, indicating a glycosidic linkage forming a (1➔3)-β-D-glucan backbone. B'''_6 was identified at 4.08, 3.55/68.9 ppm,

Table 4
Chemical shift assignments and correlations found in the NMR spectra of sample PeA3, assigned to α- and β-glucan residues, A–F. Bold indicates interresidual correlations.

Assigned monomer			δ ^{1}H (ppm)	δ ^{13}C (ppm)	HMBC	H2BC	HSQC-TOCSY	NOESY
A	→3)-α-D-Glc*p*-(1→	1	5.07	99.8	A4, A5	A2	A2, A3, A4	A2/A4, A3, **A5**, **A6**
		2	3.41	70.9	A3	A1, A3	A3, A5	
		3	3.64	82.9	A1, A2, A4	A2, A4	A2, A4, A5	A1
		4	3.41	69.6	A3, A5, A6	A3, A5	A3, A5, A6	
		5	3.83	72.1	A1, A4	A4, A6	A2, A3, A4, A6	**A1**
		6	3.63, 3.50	60.5	A4	A5	A2, A4, A5	**A1**
B′	→3)-β-D-Glc*p*-(1→	1	4.51	102.9	B′3, (**B‴3**)	B′2	B′3	B3
		2	3.29	72.6	B′3	B′1, B′3		
		3	3.49	86.7	**B‴1**, B′2, B′4	B′2, B′4	B′1	B1
		4	3.23	68.4	B′3, B′5, B′6	B′3, B′5		
		5	3.26	76.1	B′4	B′4, B′6		
		6	3.70, 3.45	60.9	B′4	B′5		
B″	→3)-β-D-Glc*p*-(1→	1	4.52	102.9	B″3, (**B‴3**)	B″2		B3
		2	3.29	72.9	B″3	B″3		
		3	3.48	86.1	B″1, B″2, B″4	B″2, B″4	B″1, B″2, B″4, B″6	B1
		4	3.23	68.4	B″3, B″5, B″6	B″3, B″5		
		5	3.26	76.4	B″4	B″4, B″6		
		6	3.70, 3.45	60.9	B″4	B″5	B″3	
B‴	→3,6)-β-D-Glc*p*-(1→	1	4.53	102.9	**B′3**	B‴2	B‴3, B‴5	B3
		2	3.33	72.7	B‴3	B‴3	B‴5	
		3	3.51	85.8	B‴1, B‴2, B‴4, **B′1**/**B″1**	B‴2, B‴4	B‴1	B1, B‴6
		4	3.27	68.5	B‴3, B‴5	B‴3, B‴5	B‴5	B‴6
		5	3.51	74.8	B‴4, B‴6	B‴4	B‴1, B‴2, B‴4, B‴6	
		6	4.07, 3.54	68.5	B‴5, **F1**		B‴5	B‴4, **F1**
C	β-D-Glc*p*-(1→	1	4.37	103.9	C2, **D3**	C2	C2, C3, C4	**D3**
		2	3.08	73.8	C1, C3	C1, C3	C1	C4
		3	3.22	76.2	C2, C6	C2	C1	
		4	3.18	70.0			C1	C2
		5						
		6	3.67, 3.43	61.1	C3			
D	→3,6)-β-D-Glc*p*-(1→	1	4.35	102.7	D2, (**E6**)	D2	D2, D3, D4	D5, (**D6**/**E6**)
		2	3.22	72.4	D1, D3	D1, D3	D1	
		3	3.41	87.2	D2, **C1**	D2, D4	D1, D2, D4	**C1**
		4	3.31	68.6		D3	D1, D3	
		5						D1
		6						
E	6)-β-D-Glc*p*-(1→	1	4.26	103.3	E6, E2	E2		E2, E3, E5, **E6**
		2	3.02	73.4	E1, E3	E1, E3	E1, E5	E1, **E5**
		3	3.19	76.4	E2	E2		E1
		4	3.14	70.0	E5	E5		**E1**, E5
		5	3.31	75.5	E4, E6	E2, E6	E1, E2, E3, E4, E6	E1, **E2**, E4, E6
		6	3.99, 3.59	68.6	E1, E5, (**D1**)	E5		**E1**, **E2**, E4, E5, (**D1**)
F	β-D-Glc*p*-(1→	1	4.22	103.0	F2, F5 **B‴6**	F2	F2, F3, F4, F5	F2, F3, F5, **B‴6**
		2	3.01	73.6	F1, F3	F1, F3	F1, F4, F6	F1, F3
		3	3.18	76.2	F2	F2	F1, F6	F1, F2
		4	3.08	70.1	F5, F6	F5	F1, F2, F6	F6
		5	3.13	76.6	F1, F4, F6	F4, F6	F1, F6	F1, F6
		6	3.68, 3.46	61.0	F4, F5	F5	F2, F3, F4, F5	F4, F5

through HMBC correlations with B'''_4 and H2BC correlations with B'''_5 and supported by an intra residue correlation between B'''_1 and B'''_6 in the HSQC-TOCSY spectrum. The higher ^{13}C chemical shift of B'''_6 indicated a glycosidic linkage and that residue B‴ was →3,6)-β-D-Glc*p*-(1→. B'''_6 shared an HMBC correlation with the *H*-1/*C*-1 cross peak of residue F indicating a glycosidic linkage between the two residues that is further confirmed by a NOESY correlation between B'''_6 and F_1 (Fig. 2B). Intra residue H2BC and HMBC correlations enabled the assignment of the remaining *H*/*C* signals from residue F as β-D-Glc*p*-(1→ attached at *O*-6 of the (1→3)-glucan backbone.

The assignment of residue E was made through H2BC and HMBC correlations and supported by HSQC-TOCSY correlations. HMBC correlations from E_1 to E_6 (4.00, 3.60/69.0 ppm) confirmed the linkage point at *O*-6, making E residues form a (1→6)-β-D-glucan backbone. The presence of inter residue NOESY correlations from E_1 to E_6 confirmed this.

C_2 and C_3 were assigned by H2BC and HMBC correlations. C_3 did not appear to participate in any glycosidic linkage. HMBC correlations from C_3 enabled the assignment of C_6 at 3.44/61.4 ppm, which was also not a linkage site. C_4 is suggested to be the signal at 3.29/70.4 ppm based on a HSQC-TOCSY correlation with C_1. C_5 was not assigned due to lack of correlations/severe overlap of correlations. Reference spectra report β-D-Glc*p*-(1→ signals to appear in the vicinity of C_1 (Abreu et al., 2021) and this assignment fits well with the current data. D_2, D_3 and D_4 were assigned through H2BC and HSQC-TOCSY correlations. D_5 and D_6 were not assigned due to lack of correlations/severe overlap of correlations. An inter residue HMBC correlation was observed between C_1 and D_3, indicating a (1→3)-glycosidic linkage between the two residues. This was further confirmed by a NOESY correlation between C_1 and D_3. The HMBC spectrum showed an inter residue correlation between *H*-(D_1) and the deshielded CH_2 carbons at ~69 ppm, indicating that residue D is (1→6)-linked, possibly to residue E. Another possible D_1/E_6 correlation was found in the NOESY spectrum (Fig. 2B). Residue D is suggested to be →3,6)-β-D-Glc*p*-(1→, which fits well with reference spectra that report anomeric signals of →3,6)-β-D-Glc*p*-(1→ to appear in the vicinity of D_1 (Abreu et al., 2021).

In addition to the characterized glucan signals, the ^{1}H spectrum also revealed an anomeric signal at around 4.9 ppm. A cross peak was found in the HSQC spectrum, at 4.92/102.2 ppm. However, the lack of HMBC and H2BC correlations made any further structure elucidation difficult.

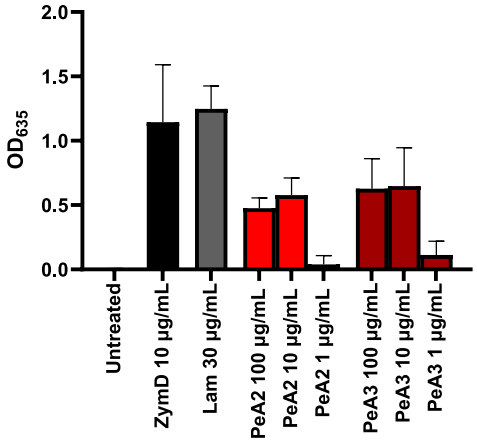

Fig. 3. β-Glucan dectin-1a binding to HEK-Blue™ hdectin-1a cells as determined by measuring the optical density at 635 nm (OD_{635}).

Based upon the results from the linkage analysis, it is possible that the signal stems from (1➔3)-linked α-D-mannose, although this has not been confirmed.

The DOSY spectrum (Fig. S8, supplementary data) provided diffusion coefficients to each of the ^{1}H resonances, thus giving an indication of which protons resided on the same molecule. However, the diffusion coefficients are dependent upon the hydrodynamic radii of the molecules in solution and is therefore related to their Mw. Because of this, protons sharing the same diffusion coefficients may either be attached to the same molecule, or they may be attached to molecules having the same Mw. Based on this, the branched (1➔3)-β-D-glucan (**2**) was found to be a separate polymer from structures **1**, **3** and **4**. Additionally, some population of residues B and F shared a diffusion coefficient with the signal at 4.92 ppm, making up another polymer. Residues A, C, D and E shared the same diffusion coefficient. It is possible that these residues belong to separate polymers, although the existence of one polymer consisting of fragments **1**, **3** and **4** cannot be ruled out. Both linear (1➔3)-α-D-glucans and branched (1➔6)-β-D-glucans are known to be found in fungi and mushrooms (Carbonero et al., 2006; Maji et al., 2012; Samuelsen et al., 2019; Synytsya & Novák, 2013). Based on this, the *P. eryngii* alkali soluble glucans are suggested to be a linear (1➔3)-α-D-glucan (**1**), a (1➔3)-β-D-glucan with single Glc*p* units attached at *O*-6 (**2**), and a (1➔6)-β-D-glucan with single Glc*p* units attached at *O*-3 (**3** + **4**).

Linear (1➔3)-α-D-glucans are known to be poorly soluble in DMSO. Accordingly, the estimated abundance of glucan **1** may be slightly too low, whereas that of glucans **2** and **3** + **4** may be slightly too high. Still, an approximation of the relative content of each of the glucans **1**, **2** and **3** + **4** in PeA3 could be calculated by integrating the ^{13}C peaks of A_3 and B'_3, B''_3, B'''_3, and combining this with the relative abundance of the various linkage types found in the methylation analysis. The results showed that **1** constituted approximately 9 %, while **2** and **3** + **4** constituted approximately 43 % and 38 % of the total sample mass, respectively.

3.2. Pro-inflammatory activity of P. eryngii glucans

Both the samples PeA2 and PeA3 were able to bind to the dectin-1 receptor at their two highest concentrations (10, 100 µg/mL), but only weakly at the lowest concentration (1 µg/mL) in the reporter cell line assay (Fig. 3). Although there was a definite binding from both samples, neither of them reached the binding levels of the positive controls.

The human monocytic cell-line THP-1 was chosen for further experiments to assess whether the dectin-1 binding correlated with proinflammatory activation. THP-1 cells have been shown to express high levels of dectin-1 after stimulation with LPS (Rogers et al., 2013) and LPS was therefore used to differentiate the cells into macrophage (Mφ)-like cells. PeA3 activated dectin-1a similarly but slightly more than PeA2 and was therefore chosen for further cell experiments. The sample was dispersed into fine particles by precipitation using different dilutions yielding PeA3-PI and PeA3-PII. This was done according to our method for dispersing poorly water-soluble β-glucans (Ellefsen et al., 2023). The previous work showed that different β-glucan dilutions yielded different particle sizes and morphology of the precipitated material. DLS measurements showed that PeA3-PII, which was produced at the highest dilution, contained a more homogeneous dispersion of smaller particles (Z-average 479 ± 81.9 nm, PDI 0.41 ± 0.1) than PeA3-PI (Z-average 1433 ± 442 nm, PDI 0.83 ± 0.16).

Treating LPS-differentiated THP-1 cells with PeA3-PI, PeA3-PII, or with the crude extract PeA3 only led to release of low to negligible amounts of TNF-α, IL-6 and IL-1β, compared to treatment with the positive control LPS and the *S. cerevisiae* particulate β-glucan controls ZymA, ZymD and BG-P. Neither of the *P. eryngii* samples led to production of statistically significant levels of any of the cytokines at any of the assayed concentrations. The same was found for the water-soluble β-glucan laminarin. The *S. cerevisiae* glucans present in both zymosan samples, and in BG-P, have been thoroughly characterized as (1➔3)-β-glucans with branching at *O*-6 (Berven et al., 2015; Gao et al., 2012). In contrast, the *P. eryngii* glucans were (1➔3)-β-D-glucan (**2**), (1➔6)-β-D-glucan (**3**–**4**), and (1➔3)-α-D-glucan (**1**). Dectin-1 is highly specific for (1➔3)-β-D-Glc*p* recognition, but is also affected by the polymer size and branching (Adams et al., 2008). As the dectin-1 expression in the THP-1 cells is likely a lot lower than in the HEK-Blue™ hDectin-1a cells, it is possible that a higher sample amount would have been needed to achieve activation in this assay, since the sample only contain about 43 % of (1➔3)-linked β-glucan. The observation that ability to activate dectin-1a did not correlate with proinflammatory activation of the Mφ-like cells could also suggest that a dual activation is necessary to achieve proper activation. However, as ZymD was able to activate the Mφ-like cells, and this product lacks activity towards TLR2, this cannot be the only explanation for the observed results.

Laminarin did not induce production of either cytokine in the cells. Laminarin is a water-soluble (1➔3)-β-D-glucan (www.sigmaaldrich.com) with few branches at *O*-6 and relatively low molecular weight (Kim et al., 2000). This indicates that to achieve proinflammatory activation in the THP-1 cells, either a more branched structure, a higher molecular weight or a particulate state is required. Laminarin has previously shown to function as an antagonist to the dectin-1 receptor in murine cells, whereas its effect on human cells has not been equally elucidated, partly due to the structural diversity of commercially available "laminarins" (Smith et al., 2018). Laminarin is able to activate the human dectin-1a receptor expressed on a reporter cell line (Ellefsen et al., 2021), but whether this will lead to cellular activation is thus still unclear.

Addition of the actin polymerization inhibitor cytochalasin D (CytD) has previously been shown to increase the release of proinflammatory cytokines from cells treated with β-glucan microparticles (Brown et al., 2003; Hernanz-Falcón et al., 2009; Rosas et al., 2008). This happens as internalization of the dectin-1 receptor is avoided due to inhibited phagocytosis. However, addition of CytD did not increase the release of the proinflammatory cytokines in the cells treated with samples or controls (Fig. 4, red bars). Interestingly, addition of CytD rather decreased the release of TNF-α and IL-1β from cells treated with BG-P. BG-P has previously been shown to be phagocytized by murine macrophage RAW264.7 cells (Berven et al., 2015). At the same time, at least a portion of BG-P is too large for phagocytosis (Ellefsen et al., 2023). BG-P would thus be expected to induce cytokine production in the absence of CytD as the largest particles would bind to the receptor but not be phagocytized. The observed reduction in cytokine production in the presence of CytD is in accordance with observations made by both Rosas et al. (2008) and Hernanz-Falcón et al. (2009). In their experiments CytD in combination with ~3 µm *S. cerevisiae* glucan microparticles (GluMP) resulted in increased cytokine production in murine dendritic

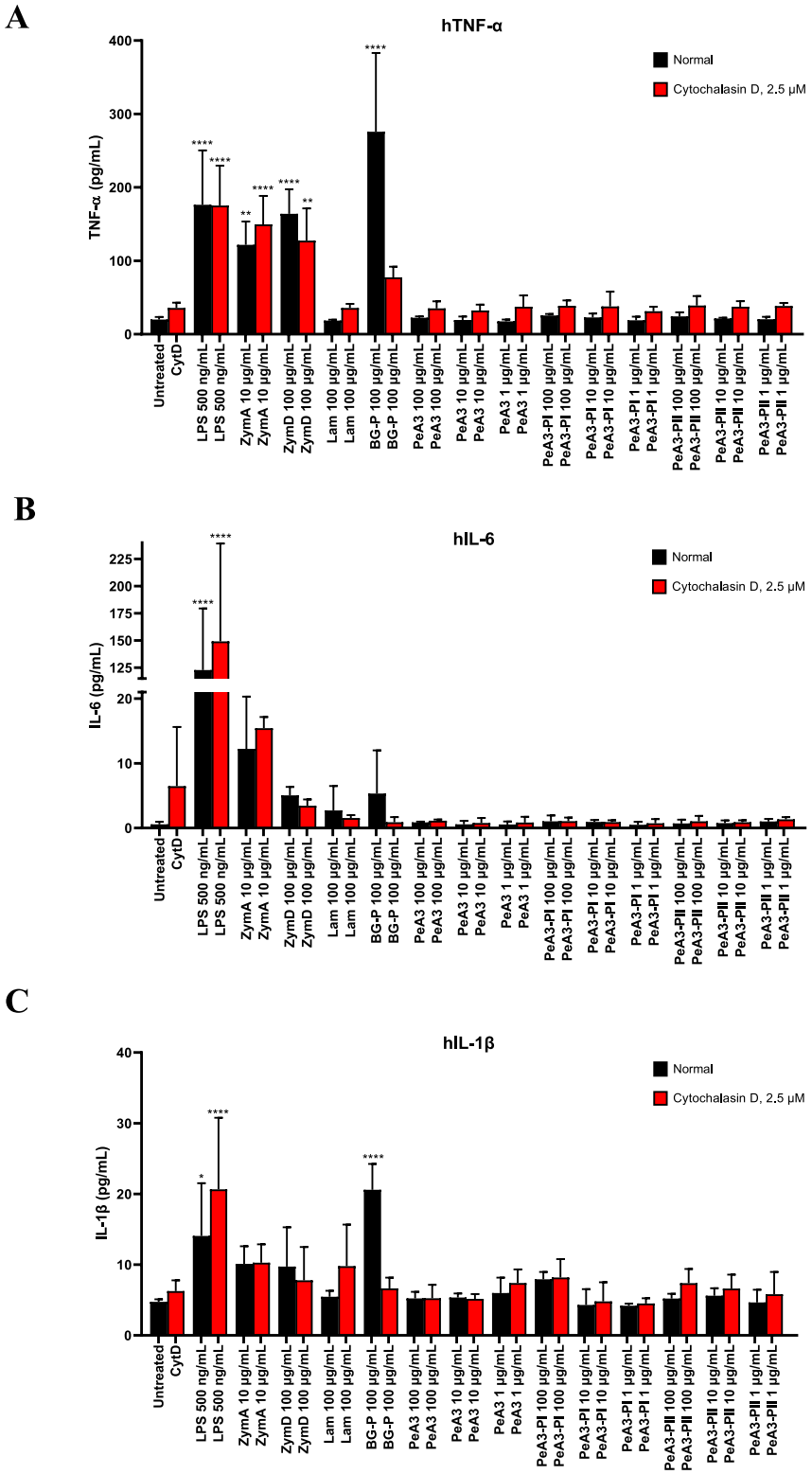

Fig. 4. Activation of LPS-differentiated THP-1 cells after incubation with *P. eryngii* alkaline extract PeA3, dispersed samples PeA3-PI and PeA3-PII, and controls as indicated by release of A TNF-α. B interleukin (IL) 6. C IL-1β. Error bars represents the SD of three series of experiments. *P < 0.0332, **P < 0.0021, ***P < 0.0002, ****P < 0.0001, as compared to the untreated control.

cells and macrophages, while cytokine production was reduced in the presence of CytD and curdlan, a (1➔3)-β-D-glucan from *Alcaligenes faecalis*, with particle sizes up to 200 μm. This was explained by limited cellular migration and accordingly limited contact between the cells and the glucan particles as a result of actin polymerization inhibition.

The measurement of LPS content is important to confirm that the β-glucan is responsible for the observed activity rather than contamination by endotoxin, and several methods for the detection or quantification of LPS in polysaccharide samples are available (de Santana-Filho et al., 2012; Rieder et al., 2013). Neither the samples nor the

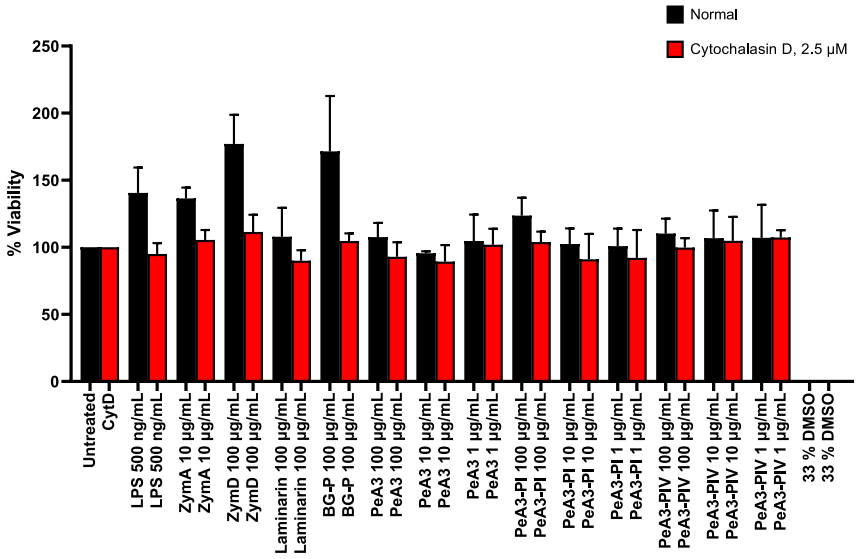

Fig. 5. Cell viability of LPS-differentiated THP-1 cells after incubation with *P. eryngii* alkaline extract PeA3, particulate samples PeA3-PI and PeA3-PII, and controls as compared to untreated cells (100 % viability) and cells treated with 33 % DMSO (0 % viability). Error bars represent the SD of three series of experiments.

β-glucan controls BG-P and laminarin contained LPS exceeding the limit of detection (0.29 ‰wt) in the current analysis. The absence of LPS in PeA3 and laminarin is also indicated by the lack of cytokine production arising from cell stimulation with these samples. BG-P induced production of both TNF-α and IL-1β at statistically significant levels. Since LPS was not detected in BG-P the activation is unlikely to be caused by contamination.

The viability of the LPS-differentiated THP-1 cells after treatment with the samples and controls was investigated. The results showed that the *P. eryngii* samples did not alter the cell viability (Fig. 5). The particulate β-glucans ZymD and BG-P seemed to increase the cell viability without CytD, indicating increased cell proliferation. None of the samples were toxic and the absence of a proinflammatory response was accordingly not caused by cell death.

4. Conclusion

The current results show that *P. eryngii* contains a mixture of alkali-soluble (1➔3) and (1➔6)-β-D-glucans, and that there are at least three structurally different polymers in the *P. eryngii* alkali extracts. These structures are likely closely associated. Despite their ability to activate the human dectin-1a receptor, the alkali-soluble glucans of *P. eryngii* lacked the ability to induce production of proinflammatory cytokines in LPS-differentiated THP-1 cells. Yeast-derived β-glucans with a (1➔3)-linked backbone and branching at *O*-6 activated the human dectin-1a receptor and induced cytokine production in the THP-1 cells. Thus, the branched (1➔3),(1➔6)-β-D-glucans from yeast seem to have more potent proinflammatory activity than the *P. eryngii* glucans.

CRediT authorship contribution statement

Christiane F. Ellefsen: Investigation, Formal analysis, Writing – original draft, Visualization. **Linda Lindstad:** Investigation. **Leesa J. Klau:** Investigation, Formal analysis. **Finn L. Aachmann:** Resources, Funding acquisition. **Marianne Hiorth:** Writing – review & editing. **Anne Berit C. Samuelsen:** Conceptualization, Supervision, Writing – review & editing.

Declaration of competing interest

The authors declare that they have no known competing financial interests or personal relationships that could have appeared to influence the work reported in this paper.

Data availability

Data will be made available on request.

Acknowledgements

The authors thank Dr. Svein H. Knutsen and Silje Johansen at NOFIMA, the Norwegian Institute of Food, Fisheries and Aquaculture Research for assistance with elemental analysis. Dr. Anne Grethe Hamre, Dept. of Pharmacy, University of Oslo is acknowledged for technical assistance. The Norwegian PhD School of Pharmacy is acknowledged for mobility funding (221832). LK, FLA were supported by the Research Council of Norway through grants 294946 (The Norwegian Seaweed Biorefinery Platform) and Norwegian NMR platform (NNP) 226244.

Appendix A. Supplementary data

Supplementary data to this article can be found online at https://doi.org/10.1016/j.carbpol.2023.121367.

References

Abreu, H., Zavadinack, M., Smiderle, F. R., Cipriani, T. R., Cordeiro, L. M. C., & Iacomini, M. (2021). Polysaccharides from *Pleurotus eryngii*: Selective extraction methodologies and their modulatory effects on THP-1 macrophages. *Carbohydrate Polymers, 252*, Article 117177.

Adams, E. L., Rice, P. J., Graves, B., Ensley, H. E., Yu, H., Brown, G. D., … Williams, D. L. (2008). Differential high-affinity interaction of dectin-1 with natural or synthetic glucans is dependent upon primary structure and is influenced by polymer chain length and side-chain branching. *Journal of Pharmacology and Experimental Therapeutics, 325*, 115–123.

Berven, L., Skjeldal, F. M., Prydz, K., Zubaidi, L. M. K., Ballance, S., Johansen, H. T., & Samuelsen, A. B. C. (2015). Particulate yeast β-glucan is internalized by RAW 264.7 macrophages and reduces the activity of the tumor-associated protease legumain. *Bioactive Carbohydrates and Dietary Fibre, 6*, 15–23.

Brown, G. D., Herre, J., Williams, D. L., Willment, J. A., Marshall, A. S. J., & Gordon, S. (2003). Dectin-1 mediates the biological effects of β-glucans. *Journal of Experimental Medicine, 197*, 1119–1124.

Carbonero, E. R., Gracher, A. H. P., Smiderle, F. R., Rosado, F. R., Sassaki, G. L., Gorin, P. A. J., & Iacomini, M. (2006). A β-glucan from the fruit bodies of edible mushrooms Pleurotus eryngii and Pleurotus ostreatoroseus. *Carbohydrate Polymers, 66*(2), 252–257.

de Santana-Filho, A. P., Noleto, G. R., Gorin, P. A. J., de Souza, L. M., Iacomini, M., & Sassaki, G. L. (2012). GC–MS detection and quantification of lipopolysaccharides in

polysaccharides through 3-O-acetyl fatty acid methyl esters. *Carbohydrate Polymers, 87*(4), 2730–2734.
Di Carlo, F., & Fiore, J. V. (1958). On the composition of zymosan. *Science, 127*, 756–757.
dos Santos, J. C., Barroso de Figueiredo, A. M., Teodoro Silva, M. V., Cirovic, B., de Bree, L. C. J., Damen, M. S. M. A., … Joosten, L. A. B. (2019). β-Glucan-induced trained immunity protects against Leishmania braziliensis infection: A crucial role for IL-32. *Cell Reports, 28*(10), 2659–2672.e2656.
DuBois, M., Gilles, K. A., Hamilton, J. K., Rebers, P. A., & Smith, F. (1956). Colorimetric method for determination of sugars and related substances. *Analytical Chemistry, 28*(3), 350–356.
Ellefsen, C. F., Struzek, A.-M., Scherließ, R., Hiorth, M., & Samuelsen, A. B. C. (2023). Preparation of Albatrellus ovinus β-glucan microparticles with dectin-1a binding properties. *ACS Applied Bio Materials, 6*(5), 1863–1872.
Ellefsen, C. F., Wold, C. W., Wilkins, A. L., Rise, F., & Samuelsen, A. B. C. (2021). Water-soluble polysaccharides from Pleurotus eryngii fruiting bodies, their activity and affinity for Toll-like receptor 2 and dectin-1. *Carbohydrate Polymers, 264*, Article 117991.
Ferwerda, G., Meyer-Wentrup, F., Kullberg, B.-J., Netea, M. G., & Adema, G. J. (2008). Dectin-1 synergizes with TLR2 and TLR4 for cytokine production in human primary monocytes and macrophages. *Cellular Microbiology, 10*(10), 2058–2066.
Gantner, B. N., Simmons, R. M., Canavera, S. J., Akira, S., & Underhill, D. M. (2003). Collaborative induction of inflammatory responses by dectin-1 and Toll-like receptor 2. *Journal of Experimental Medicine, 197*(9), 1107–1117.
Gao, Y., Jiang, R., Qie, J., Chen, Y., Xu, D., Liu, W., & Gao, Q. (2012). Studies on the characteristic and activity of low-molecular fragments from zymosan. *Carbohydrate Polymers, 90*(4), 1411–1414.
Graubaum, H.-J., Busch, R., Stier, H., & Gruenwald, J. (2012). A double-blind, randomized, placebo-controlled nutritional study using an insoluble yeast beta-glucan to improve the immune defense system. *Food and Nutrition Sciences, 3*, 738–746.
Han, B., Baruah, K., Cox, E., Vanrompay, D., & Bossier, P. (2020). Structure-functional activity relationship of β-glucans from the perspective of immunomodulation: A mini-review. *Frontiers in Immunology, 11*(658) (Mini Review).
Hernanz-Falcón, P., Joffre, O., Williams, D. L., & Reis e Sousa, C.. (2009). Internalization of Dectin-1 terminates induction of inflammatory responses. *European Journal of Immunology, 39*(2), 507–513.
Kim, Y.-T., Kim, E.-H., Cheong, C., Williams, D. L., Kim, C.-W., & Lim, S.-T. (2000). Structural characterization of β-d-(1→3, 1→6)-linked glucans using NMR spectroscopy. *Carbohydrate Research, 328*(3), 331–341.
Maji, P. K., Sen, I. K., Behera, B., Maiti, T. K., Mallick, P., Sikdar, S. R., & Islam, S. S. (2012). Structural characterization and study of immunoenhancing properties of a glucan isolated from a hybrid mushroom of Pleurotus florida and Lentinula edodes. *Carbohydrate Research, 358*, 110–115.
Nyman, A. A. T., Aachmann, F. L., Rise, F., Ballance, S., & Samuelsen, A. B. C. (2016). Structural characterization of a branched (1→6)-α-mannan and β-glucans isolated from the fruiting bodies of Cantharellus cibarius. *Carbohydrate Polymers, 146*, 197–207.
Pettolino, F. A., Walsh, C., Fincher, G. B., & Bacic, A. (2012). Determining the polysaccharide composition of plant cell walls. *Nature Protocols, 7*(9), 1590–1607.
Rieder, A., Grimmer, S., Aachmann, L., Westereng, F. B., Kolset, S. O., & Knutsen, S. H. (2013). Generic tools to assess genuine carbohydrate specific effects on in vitro immune modulation exemplified by β-glucans. *Carbohydrate Polymers, 92*(2), 2075–2083.
Rogers, H., Williams, D. W., Feng, G.-J., Lewis, M. A. O., & Wei, X.-Q. (2013). Role of bacterial lipopolysaccharide in enhancing host immune response to Candida albicans. *Clinical and Developmental Immunology, 2013*, Article 320168.
Rosas, M., Liddiard, K., Kimberg, M., Faro-Trindade, I., McDonald, J. U., Williams, D. L., … Taylor, P. R. (2008). The induction of inflammation by dectin-1 in vivo is dependent on myeloid cell programming and the progression of phagocytosis. *The Journal of Immunology, 181*, 3549–3557.
Rösch, C., Meijerink, M., Delahaije, R. J. B. M., Taverne, N., Gruppen, H., Wells, J. M., & Schols, H. A. (2016). Immunomodulatory properties of oat and barly β-glucan populations on bone marrow derived dendritic cells. *Journal of Functional Foods, 26*, 279–289.
Ruiz-Herrera, J., & Ortiz-Castellanos, L. (2019). Cell wall glucans of fungi. A reiview. *The Cell Surface, 5*, Article 100022.
Samuelsen, A. B. C., Rise, F., Wilkins, A. L., Teveleva, L., Nyman, A. A. T., & Aachmann, F. L. (2019). The edible mushroom Albatrellus ovinus contains a α-L-fuco-α-D-galactan, α-D-glucan, a branched (1→6)-β-D-glucan and a branched (1→3)-β-D-glucan. *Carbohydrate Research, 471*, 28–38.
Smith, A. J., Graves, B., Child, R., Rice, P. J., Ma, Z., Lowman, D. W., … Williams, D. L. (2018). Immunoregulatory activity of the natural product laminarin varies widely as a result of its physical properties. *The Journal of Immunology, 200*(2), 788–799.
Synytsya, A., & Novák, M. (2013). Structural diversity of fungal glucans. *Carbohydrate Polymers, 92*(1), 792–809.
Vetvicka, V., Vannucci, L., & Sima, P. (2020). β-Glucan as a new tool in vaccine development. *Scandinavian Journal of Immunology, 91*(2), Article e12833.
Williams, D. L., Mueller, A., & Browder, W. (1996). Glucan-based macrophage stimulators. *Clinical Immunotherapeutics, 5*(5), 392–399.
Zhang, Y., Li, S., Wang, X., Zhang, L., & Cheung, P. C. K. (2011). Advances in lentinan: Isolation, structure, chain conformation and bioactivities. *Food Hydrocolloids, 25*(2), 196–206.